# Vector Precoding in Wireless Communications: A Replica Symmetric Analysis

Invited Paper

Ralf R. Müller
Norwegian University of Science and Technology
IET
7491 Trondheim, Norway
ralf@iet.ntnu.no

Dongning Guo
Northwestern University
Dept EECS
Evanston, IL, U.S.A.
dGuo@northwestern.edu

Aris L. Moustakas
National and Kapodistrian University of Athens
Physics Dept
Athens, Greece
arislm@phys.uoa.gr

## ABSTRACT

We apply the replica method to analyze vector pre-coding, a method to reduce transmit power in antenna array communications, in the limit of an infinite number of dimensions of the signal vector. The analysis applies to a very general class of channel matrices. The statistics of the channel matrix enter the transmitted energy per symbol via its R-transform.

## Categories and Subject Descriptors

H.4 [**Information Systems Applications**]: Miscellaneous

## General Terms

Wireless communications, statistical mechanics

## 1. INTRODUCTION

Vector precoding aims to minimize the transmitted power that is associated with the transmission of a certain data vector $\boldsymbol{s} \in \mathcal{S}^K$ of length $K$. For that purpose, the original symbol alphabet $\mathcal{S}$ is relaxed into the alphabet $\mathcal{B}$. The data representation in the relaxed alphabet is redundant. That means that several symbols in the relaxed alphabet represent the same data. Due to the redundant representation, we can now choose that representation of our data which requires the least power to be transmitted. This way of saving transmit power is called vector pre-coding.

That means, for any $s_k \in \mathcal{S}$, e.g. $\mathcal{S} = \{1, 0\}$, there is a set $\mathcal{B}_{s_k} \subset \mathcal{B}$, e.g. $\mathcal{B} = \mathbb{Z}$, such that all elements of $\mathcal{B}_{s_k}$ represent the data $s_k$. For binary transmission without vector pre-coding, it is most common to choose $\mathcal{B}_0 = \{+1\}$ and $\mathcal{B}_1 = \{-1\}$. This modulation is called binary phase shift keying. For binary modulation, vector pre-coding is the idea to allow for supersets of $\mathcal{B}_0$ and $\mathcal{B}_1$.


Valuetools '07, October 23-25, 2007, Nantes, France.


In order to avoid ambiguities, we should have

$$\mathcal{B}_i \cap \mathcal{B}_j = \emptyset \qquad \forall i \neq j. \tag{1}$$

In addition, one would like to design the sets $\mathcal{B}_i$ such that the distance properties between the presented information are preserved. This is easily achieved by letting the sets $\mathcal{B}_i$ to be distinct sub-lattices of $\mathcal{B}$. However, we are not concerned with these design issues here. We aim to analyze the power saving achieved by a particular choice of the sets $\mathcal{B}_i$. This goal is achieved using the replica method invented in statistical physics.

The replica method was introduced into multiuser communications by the landmark paper of Tanaka [15] for the purpose of studying the performance of the maximum a-posteriori detector. Subsequently his work was generalized and extended other problems in multiuser communications by himself and Saad [17], Guo and Verdú [4], Müller et al. [14, 13], Caire et al. [1], Tanaka and Okada [16], Kabashima [8], Li and Poor [9], Guo [3], and Wen and Wong [21]. Additionally, the replica method has also been successfully used for the design and analysis of error correction codes. Vector pre-coding has been discussed in the non-asymptotic regime by several authors, e.g. [6]

## 2. PROBLEM STATEMENT

Let $\boldsymbol{s}$ denote the information to be encoded. Let $\boldsymbol{t} = \boldsymbol{T}\boldsymbol{x}$ be the vector being sent. Then, the pre-coding problem can be written as the minimization of the following quadratic form

$$\min_{\boldsymbol{x} \in \mathcal{X}} \boldsymbol{x}^\dagger \boldsymbol{R} \boldsymbol{x} \tag{2}$$

over the discrete set

$$\mathcal{X} = \mathcal{B}_{s_1} \times \mathcal{B}_{s_2} \times \cdots \times \mathcal{B}_{s_K} \tag{3}$$

with $\boldsymbol{R} = \boldsymbol{T}^\dagger \boldsymbol{T}$ with $s_1, s_2, \ldots, s_K$ representing the information sequence to be encoded.

In order to allow for analytical tractability, we need a few assumptions:

Assumption 1 (self-averaging property). *We have*

$$\lim_{K \to \infty} \Pr\left( \frac{1}{K} \left| \min_{\boldsymbol{x} \in \mathcal{X}} \boldsymbol{x}^\dagger \boldsymbol{R} \boldsymbol{x} - \mathop{\mathrm{E}}_{\boldsymbol{R}} \min_{\boldsymbol{x} \in \mathcal{X}} \boldsymbol{x}^\dagger \boldsymbol{R} \boldsymbol{x} \right| > \epsilon \right) = 0 \tag{4}$$

*for all $\epsilon > 0$, i.e. convergence in probability.*

ASSUMPTION 2 (REPLICA CONTINUITY). *For all $\beta > 0$, the continuation of the function*

$$f(n) = \prod_{a=1}^{n} \sum_{\boldsymbol{x}_a \in \mathcal{X}} \mathrm{e}^{-\beta \boldsymbol{x}_a^\dagger \boldsymbol{R} \boldsymbol{x}_a} \tag{5}$$

*onto the positive real line is equal to*

$$\left( \sum_{\boldsymbol{x} \in \mathcal{X}} \mathrm{e}^{-\beta \boldsymbol{x}^\dagger \boldsymbol{R} \boldsymbol{x}} \right)^n$$

*in the vicinity of $n = 0$.*

ASSUMPTION 3 (UNITARY INVARIANCE). *The random matrix $\boldsymbol{R}$, can be decomposed into*

$$\boldsymbol{R} = \boldsymbol{O}\boldsymbol{D}\boldsymbol{O}^\dagger \tag{6}$$

*such that the matrices $\boldsymbol{D}$ and $\boldsymbol{O}$ are diagonal and Haar distributed, respectively. Moreover, as $K \to \infty$, the asymptotic eigenvalue distribution of $\boldsymbol{R}$ converges to a non-random distribution function which can be uniquely characterized by its R-transform[1] $R(w)$.*

ASSUMPTION 4 (REPLICA SYMMETRY). *When applying the replica method to solve the saddle-point equations, we will assume that the extremal point is invariant to permutations of the replica index. For a detailed discussion of replica symmetry, the reader is referred to the literature of spin glasses, e.g. [11].*

The first three assumptions are rather technical and should hold well in the application we are addressing. The validity of replica symmetry, by contrast, is a postulate which, for sake of analytical tractability, is made without further justification.

## 3. GENERAL RESULT

With the previous assumptions, we find for the average transmitted energy per symbol in the large system limit

$$\begin{aligned}
E_\mathrm{s} &= \lim_{K\to\infty} \frac{1}{K} \min_{\boldsymbol{x}\in\mathcal{X}} \boldsymbol{x}^\dagger \boldsymbol{R} \boldsymbol{x} && (7)\\
&= -\lim_{K\to\infty} \lim_{\beta\to\infty} \frac{1}{\beta K} \mathop{\mathrm{E}}_{\boldsymbol{R}} \log \sum_{\boldsymbol{x}\in\mathcal{X}} \mathrm{e}^{-\beta \boldsymbol{x}^\dagger \boldsymbol{R} \boldsymbol{x}} && (8)\\
&= -\lim_{K\to\infty} \lim_{\beta\to\infty} \frac{1}{\beta K} \lim_{n\to 0} \frac{\partial}{\partial n} \log \mathop{\mathrm{E}}_{\boldsymbol{R}} \left( \sum_{\boldsymbol{x}\in\mathcal{X}} \mathrm{e}^{-\beta \boldsymbol{x}^\dagger \boldsymbol{R} \boldsymbol{x}} \right)^n && (9)\\
&= -\lim_{\beta\to\infty} \frac{1}{\beta} \lim_{n\to 0} \frac{\partial}{\partial n} \underbrace{\lim_{K\to\infty} \frac{1}{K} \log \mathop{\mathrm{E}}_{\boldsymbol{R}} \prod_{a=1}^{n} \sum_{\boldsymbol{x}_a\in\mathcal{X}} \mathrm{e}^{-\beta \boldsymbol{x}_a^\dagger \boldsymbol{R} \boldsymbol{x}_a}}_{\triangleq \Xi_n}.
\end{aligned}$$

where the argument of the logarithm in (10) is given by

$$\begin{aligned}
\Xi_n &= \lim_{K\to\infty} \frac{1}{K} \log \mathop{\mathrm{E}}_{\boldsymbol{R}} \sum_{\{\boldsymbol{x}_a\in\mathcal{X}\}} \exp\left[ -\beta \sum_{a=1}^{n} \boldsymbol{x}_a^\dagger \boldsymbol{R} \boldsymbol{x}_a \right] && (10)\\
&= \lim_{K\to\infty} \frac{1}{K} \log \mathop{\mathrm{E}}_{\boldsymbol{R}} \sum_{\{\boldsymbol{x}_a\in\mathcal{X}\}} \exp\left[ \mathrm{tr}\left( -\beta \boldsymbol{R} \sum_{a=1}^{n} \boldsymbol{x}_a \boldsymbol{x}_a^\dagger \right) \right].
\end{aligned}$$

[1] See [20, 12, 19] for the definition of the R-transform.

Using Assumption 3, we can integrate over the Haar distributed eigenvectors of $\boldsymbol{R}$. Let $R(w)$ denote the R-transform [20] of the asymptotic eigenvalue distribution of $\boldsymbol{R}$. Then, we have from [10, 7]

$$\Xi_n = \lim_{K\to\infty} \frac{1}{K} \log \sum_{\{\boldsymbol{x}_a\in\mathcal{X}\}} \exp\left[ -K \sum_{a=1}^{n} \int_0^1 \lambda_a R(-\lambda_a w) dw \right] \tag{11}$$

with $\lambda_i$ denoting the $n$ positive eigenvalues of

$$\beta \sum_{a=1}^{n} \boldsymbol{x}_a \boldsymbol{x}_a^\dagger. \tag{12}$$

In their original work [10], Marinari et al. do not formulate their result in terms of the R-transform from free probability theory, but in terms of what they call the *generating function*. The equivalence of our and their formulation is shown in Appendix A.

The eigenvalues $\lambda_i$ are completely determined by the inner products

$$K Q_{ab} = \boldsymbol{x}_a^\dagger \boldsymbol{x}_b \triangleq \sum_{k=1}^{K} x_{ak}^* x_{bk}. \tag{13}$$

In order to perform the summation in (11), the $Kn$-dimensional space spanned by the replicas is split into subshells

$$S\{Q\} \triangleq \left\{ \boldsymbol{x}_1, \ldots, \boldsymbol{x}_n \,\middle|\, \boldsymbol{x}_a^\dagger \boldsymbol{x}_b = K Q_{ab} \right\} \tag{14}$$

where the inner product of two different replicated vectors $\boldsymbol{x}_a$ and $\boldsymbol{x}_b$ is constant.[2] With this splitting of the space, we find[3]

$$\Xi_n = \lim_{K\to\infty} \frac{1}{K} \log \int_{\mathbb{R}^{n^2}} \mathrm{e}^{K\mathcal{I}\{Q\}} \mathrm{e}^{-K\mathcal{G}\{Q\}} \prod_{a,b} \mathrm{d}Q_{ab}, \tag{15}$$

where

$$\mathrm{e}^{K\mathcal{I}\{Q\}} = \int \prod_{a=1}^{n} \left[ \prod_{b=1}^{n} \delta\left( \boldsymbol{x}_a^\dagger \boldsymbol{x}_b - K Q_{ab} \right) \right] \mathrm{dP}_{\boldsymbol{x}}(\boldsymbol{x}_a) \tag{16}$$

denotes the probability weight of the subshell and

$$\begin{aligned}
\mathcal{G}\{Q\} &= \sum_{a=1}^{n} \int_0^1 \lambda_a\{Q\} R\big( -\lambda_a\{Q\} w \big) \,\mathrm{d}w && (17)\\
&= \sum_{a=1}^{n} \int_0^{\lambda_a\{Q\}} R(-w) \,\mathrm{d}w && (18)
\end{aligned}$$

This procedure is a change of integration variables in multiple dimensions where the integration of an exponential function over the replicas has been replaced by integration over the variables $\{Q\}$. In the following the two exponential terms in (15) are evaluated separately.

First, we turn to the evaluation of the measure $\mathrm{e}^{K\mathcal{I}\{Q\}}$. Since for some $t \in \mathbb{R}$, we have the Fourier expansion of

[2] The notation $f\{Q\}$ expresses dependency of the function $f(\cdot)$ on $Q_{ab}, 1 \le a \le b \le n$.

[3] The notation $\prod_{a,b}$ is used as shortcut for $\prod_{a=1}^{n} \prod_{b=1}^{n}$.

the Dirac measure

$$\delta\left(\boldsymbol{x}_a^\dagger \boldsymbol{x}_b - KQ_{ab}\right) = \int_{\mathcal{J}} \exp\left[\tilde{Q}_{ab}\left(\boldsymbol{x}_a^\dagger \boldsymbol{x}_b - KQ_{ab}\right)\right] \frac{\mathrm{d}\tilde{Q}_{ab}}{2\pi\mathrm{j}} \tag{19}$$

with $\mathcal{J} = (t - \mathrm{j}\infty; t + \mathrm{j}\infty)$, the measure $\mathrm{e}^{K\mathcal{I}\{Q\}}$ can be expressed as

$$\begin{aligned} \mathrm{e}^{K\mathcal{I}\{Q\}} &= \int \left[\prod_{a,b} \int_{\mathcal{J}} \mathrm{e}^{\tilde{Q}_{ab}\left(\boldsymbol{x}_a^\dagger \boldsymbol{x}_b - KQ_{ab}\right)} \frac{\mathrm{d}\tilde{Q}_{ab}}{2\pi\mathrm{j}}\right] \prod_{a=1}^{n} \mathrm{dP}_{\boldsymbol{x}}(\boldsymbol{x}_a) \\ &= \int_{\mathcal{J}^{n^2}} \mathrm{e}^{\log \prod_{k=1}^{K} M_k\left\{\tilde{Q}\right\} - K \sum_{a,b} \tilde{Q}_{ab} Q_{ab}} \prod_{a,b} \frac{\mathrm{d}\tilde{Q}_{ab}}{2\pi\mathrm{j}} \end{aligned} \tag{20}$$

with

$$M_k\left\{\tilde{Q}\right\} = \int \exp\left(\sum_{a,b} \tilde{Q}_{ab} x_a^* x_b\right) \prod_{a=1}^{n} \mathrm{dP}_{x_k}(x_a). \tag{21}$$

In the limit of $K \to \infty$ one of the exponential terms in (15) will dominate over all others. Thus, only the maximum value of the correlation $Q_{ab}$ is relevant for calculation of the integral.

At this point, we assume replica symmetry. This means, that in order to find the maximum of the objective function, we consider only a subset of the potential possibilities that the variables $Q_{ab}$ could take. Here, we restrict them to the following two different possibilities $Q_{ab} = q, \forall a \neq b$ and $Q_{aa} = q + b/\beta, \forall a$. One case distinction has been made to distinguish correlations $Q_{ab}$ which correspond to correlations between different and identical replica indices, respectively. We apply the same idea to the correlation variables in the Fourier domain and set with a modest amount of foresight $\tilde{Q}_{ab} = \beta^2 f^2/2, \forall a \neq b$ and $\tilde{Q}_{aa} = \beta^2 f^2/2 - \beta e, \forall a$. Note that the matrix defined by $Q_{ab}$ is positive semidefinite. This implies that the replica symmetric parameters $q, b, f, e$ are all real.

At this point the crucial benefit of the replica method becomes obvious. Assuming replica continuity, we have managed to reduce the evaluation of a continuous function to sampling it at integer points. Assuming replica symmetry we have reduced the task of evaluating infinitely many integer points to calculating four different correlations (two in the original and two in the Fourier domain).

The assumption of replica symmetry leads to

$$\sum_{a,b} \tilde{Q}_{ab} Q_{ab} = \frac{n(n-1)}{2} \beta^2 f^2 q + n\left(\frac{\beta f^2}{2} - e\right)(\beta q + b) \tag{22}$$

and

$$M_k(e,f) = \int \mathrm{e}^{\frac{\beta}{2} \sum_{a=1}^{n} (\beta f^2 - 2e)|x_a|^2 + 2 \sum_{b=a+1}^{n} \beta f^2 \Re\left\{x_a^* x_b\right\}} \times \times \prod_{a=1}^{n} \mathrm{dP}_{x_k}(x_a) \tag{23}$$

Note that the prior distribution enters the free energy only via (23). We will focus on this later on after having finished with the other terms.

For the evaluation of $\mathcal{G}\{Q\}$ in (15), we can use the replica symmetry to explicitly calculate the eigenvalues $\lambda_i$. Considerations of linear algebra lead to the conclusion that the eigenvalues $b$ and $b + \beta nq$ occur with multiplicities $n-1$ and 1, respectively. Thus we get

$$\mathcal{G}(q,b) = (n-1) \int_0^b R(-w)\,\mathrm{d}w + \int_0^{b+\beta nq} R(-w)\,\mathrm{d}w \tag{24}$$

Since the integral in (15) is dominated by the maximum argument of the exponential function, the derivatives of

$$\mathcal{G}\{Q\} + \sum_{a,b} \tilde{Q}_{ab} Q_{ab} \tag{25}$$

with respect to $q$ and $b$ must vanish as $K \to \infty$. Taking derivatives after plugging (22) and (24) into (25), gives

$$\begin{aligned} \beta n R(-b - \beta nq) + \frac{n(n-1)}{2} \beta^2 f^2 + \beta n \left(\frac{\beta f^2}{2} - e\right) &= 0 \\ (n-1) R(-b) + R(-b - \beta nq) + n\left(\frac{\beta f^2}{2} - e\right) &= 0 \end{aligned}$$

solving for $e$ and $f$ gives

$$e = R(-b) \tag{26}$$

$$f = \sqrt{2 \frac{R(-b) - R(-b - \beta nq)}{\beta n}} \tag{27}$$

with the limits for $n \to 0$

$$f \overset{n \to 0}{\longrightarrow} \sqrt{2qR'(-b)} \tag{28}$$

$$n \frac{\mathrm{d}f}{\mathrm{d}n} \overset{n \to 0}{\longrightarrow} 0. \tag{29}$$

Consider now the integration over the prior distribution in the moment-generating function. Consider (23) giving the only term that involves the prior distribution and apply the complex Hubbard-Stratonovich transform

$$\mathrm{e}^{\frac{|x|^2}{2}} = \frac{1}{2\pi} \int_{\mathbb{C}} \mathrm{e}^{\pm\Re\{xz^*\} - \frac{|z|^2}{2}} \mathrm{d}z =: \int \mathrm{e}^{\pm\Re\{xz\}} \mathrm{D}z. \tag{30}$$

Then, we find with (23)

$$\begin{aligned} M_k(e,f) &= \int \mathrm{e}^{\frac{\beta^2 f^2}{2} \left|\sum_{a=1}^{n} x_a\right|^2 - \sum_{a=1}^{n} \beta e |x_a|^2} \prod_{a=1}^{n} \mathrm{dP}_{x_k}(x_a) \\ &= \iint \mathrm{e}^{\beta \sum_{a=1}^{n} f \Re\left\{x_a z^*\right\} - e|x_a|^2} \mathrm{D}z \prod_{a=1}^{n} \mathrm{dP}_{x_k}(x_a) \\ &= \int \left(\int \mathrm{e}^{\beta f \Re\{xz^*\} - \beta e |x|^2} \mathrm{dP}_{x_k}(x)\right)^n \mathrm{D}z \end{aligned} \tag{31}$$

Moreover, for $K \to \infty$, we have by the law of large numbers

$$\begin{aligned} \log M(e,f) &= \frac{1}{K} \log \prod_{k=1}^{K} M_k(e,f) \\ &= \int \log \int \left(\int \mathrm{e}^{\beta f \Re\{z^* x\} - \beta e |x|^2} \mathrm{dP}_{x_k}(x)\right)^n \mathrm{D}z \mathrm{dP}_s(x_k)\,. \end{aligned} \tag{32}$$

In the large system limit, the integral in (20) is dominated by that value of the integration variable which maximizes

the argument of the exponential function. Thus, partial derivatives of

$$\log M(e,f) - \frac{n(n-1)}{2} f^2\beta^2 q - n\left(\frac{\beta f^2}{2} - e\right)(b+\beta q) \quad (33)$$

with respect to $f$ and $e$ must vanish as $K \to \infty$.

An explicit calculation of the two derivatives gives the following expressions for the macroscopic parameters $q$ and $b$

$$b \overset{n\to 0}{\longrightarrow} \frac{1}{f}\iint \frac{\int \Re\{z^* x\} \mathrm{e}^{\beta f \Re\{z^* x\} - \beta e |x|^2} \mathrm{dP}_{x_k}(x)}{\int \mathrm{e}^{\beta f \Re\{z^* x\} - \beta e |x|^2} \mathrm{dP}_{x_k}(x)} \mathrm{D}z \, \mathrm{dP}_s(x_k)$$

$$q \overset{n\to 0}{\longrightarrow} \iint \frac{\int |x|^2 \mathrm{e}^{\beta f \Re\{z^* x\} - \beta e |x|^2} \mathrm{dP}_{x_k}(x)}{\int \mathrm{e}^{\beta f \Re\{z^* x\} - \beta e |x|^2} \mathrm{dP}_{x_k}(x)} \mathrm{D}z \mathrm{dP}_s(x_k) - \frac{b}{\beta}.$$

Moreover, we find

$$\lim_{n\to 0} \frac{\mathrm{d}b}{\mathrm{d}n} = 0 \quad (34)$$

Returning to our initial goal, the evaluation of the average transmitted energy per symbol, and collecting our previous results, we find

$$\begin{aligned} E_\mathrm{s} &= -\lim_{\beta\to\infty}\frac{1}{\beta}\lim_{n\to 0}\frac{\partial}{\partial n}\Xi_n & (35)\\ &= \lim_{\beta\to\infty}\frac{1}{\beta}\lim_{n\to 0}\frac{\partial}{\partial n}(n-1)\int_0^b R(-w)\,\mathrm{d}w + \int_0^{b+\beta n q} R(-w)\,\mathrm{d}w \\ &\quad - \log M(e,f) + \tfrac{n(n-1)}{2} f^2\beta^2 q + \tfrac{n}{2}(f^2\beta - 2e)(b+\beta q) \\ &= \lim_{\beta\to\infty}\frac{1}{\beta}\int_0^b R(-w)\,\mathrm{d}w - bR(-b) + \beta q b R'(-b) & (36)\\ &\quad -\frac{1}{\beta}\iint \log \int \mathrm{e}^{\beta f \Re\{z^* x\} - \beta e |x|^2} \mathrm{dP}_{x_k}(x)\, \mathrm{D}z\, \mathrm{dP}_s(x_k) \\ &= \lim_{\beta\to\infty} R(-b)\left(q + \frac{b}{\beta}\right) - qbR'(-b) & (37) \end{aligned}$$

where the last equality follows from l'Hospital's rule and the re-substitutions of $b$ and $q$ applying (34) and (34). Note that for any bound on the amplitude of the signal set $\mathcal{B}$, the parameter $q$ is finite. Even without bound, $q$ will remain finite for a well-defined minimization problem. The parameter $b$ behaves in a more complicated manner. It can be both zero, finite, and infinite as $\beta \to \infty$ depending on the particular R-transform.

Consider now the most interesting case $0 < b < \infty$ for $\beta \to \infty$. First, this implies with (34) that

$$\begin{aligned} q &\overset{\beta\to\infty}{\longrightarrow} \lim_{\beta\to\infty}\iint \frac{\int |x|^2 \mathrm{e}^{\beta f \Re\{z^* x\} - \beta e |x|^2} \mathrm{dP}_{x_k}(x)}{\int \mathrm{e}^{\beta f \Re\{z^* x\} - \beta e |x|^2} \mathrm{dP}_{x_k}(x)} \mathrm{D}z \mathrm{dP}_s(x_k) \\ &= \iint \left| \operatorname*{argmin}_{x\in\mathcal{B}_{x_k}} \left| z\sqrt{\frac{qR'(-b)}{2R^2(-b)}} - x \right| \right|^2 \mathrm{D}z \mathrm{dP}_s(x_k) \quad (38) \end{aligned}$$

Second, we find

$$b \overset{\beta\to\infty}{\longrightarrow} \iint \Re\left\{ \operatorname*{argmin}_{x\in\mathcal{B}_{x_k}} \left| z\sqrt{\frac{qR'(-b)}{2R(-b)^2}} - x \right| z^* \right\} \frac{\mathrm{D}z \mathrm{dP}_s(x_k)}{\sqrt{2qR'(-b)}}$$

Note that the minimization with respect to the symbol $x$ splits the integration space of $z$ into the Voronoi regions defined by the (appropriately scaled) signal constellation $\mathcal{B}_{x_k}$. Finally, the energy per symbol simplifies to

$$\begin{aligned} E_\mathrm{s} &= qR(-b) - qbR'(-b) & (39)\\ &= q\frac{\partial}{\partial b} bR(-b) & (40)\\ &= q\frac{\partial}{\partial b} bm^{-1}(b) & (41)\\ &= q\left(s + \frac{m(s)}{m'(s)}\right) & (42) \end{aligned}$$

with $b = m(s)$ being the Stieltjes transform of the asymptotic eigenvalue distribution.

# 4. PARTICULAR RANDOM MATRICES

The general result leaves us with two objects to specify: 1) The statistics of the random matrix entering the energy per symbol via its R-transform. 2) The relaxed signal alphabets $\mathcal{B}_i \, \forall i \in \mathcal{S}$. While the relaxed alphabets characterize a particular method of pre-coding, the random matrix statistics depends on the wireless communication system. In the following, we will consider two choices for the statistics of the random matrix.

## 4.1 Zero-Forcing Transmission

Consider a vector-valued communication system. Let the received vector be given as

$$\boldsymbol{r} = \boldsymbol{H}\boldsymbol{t} + \boldsymbol{n} \quad (43)$$

where $\boldsymbol{n}$ is white Gaussian noise. Let the components of the transmitted and received vectors be signals sent and received at different antenna elements, respectively.

We now want to ensure that the received signal is (up to additive noise) identical to the data vector. This design criteria leads us to choose

$$\boldsymbol{T} = \boldsymbol{H}^\dagger \left(\boldsymbol{H}\boldsymbol{H}^\dagger\right)^{-1}. \quad (44)$$

This means that we invert the channel and get $\boldsymbol{r} = \boldsymbol{x} + \boldsymbol{n}$ if the matrix inverse exists. This allows to keep the signal processing at the receiver at a minimum. This is advantageous if the receiver shall be a low-cost or battery-powered device.

To model the statistics of the entries of $\boldsymbol{H}$ is a non-trivial task and a topic of ongoing research, see e.g. [2] and references therein. For sake of convenience, we choose in this first order approach that the entries of the channel matrix $\boldsymbol{H}$ are independent and identically distributed complex Gaussian random variables with zero mean and variance $1/N$.

## 4.2 Marchenko-Pastur Kernel

The kernel for channel inversion leads to a rather complicated R-transform. In order to build up better intuition into the mathematical structure of these kinds of combinatorial optimization problems, we also consider the case where the random matrix follows the Marchenko-Pastur law which has a very simple R-transform.

## 5. 1-D LATTICE

Consider now the following case:

$$\mathcal{S} = \{0,1\} \quad (45)$$

$$\mathcal{B}_1 = -\mathcal{B}_0 \subset \mathbb{R} \quad (46)$$

Then, we find in the limit $\beta \to \infty$

$$q = \int_{\mathbb{R}} \left| \operatorname*{argmin}_{x\in\mathcal{B}_1} \left| z\sqrt{\frac{qR'(-b)}{2R^2(-b)}} - x \right| \right|^2 \frac{\mathrm{e}^{-\frac{z^2}{2}}\,\mathrm{d}z}{\sqrt{2\pi}} \quad (47)$$

$$b = \int_{\mathbb{R}} \operatorname*{argmin}_{x\in\mathcal{B}_1} \left| z\sqrt{\frac{qR'(-b)}{2R^2(-b)}} - x \right| \frac{z\,\mathrm{e}^{-\frac{z^2}{2}}\,\mathrm{d}z}{\sqrt{4\pi qR'(-b)}}. \quad (48)$$

Moreover, let without loss of generality $-\infty = c_0 < c_1 < \cdots < c_L < c_{L+1} = +\infty$ and

$$\mathcal{B}_1 = \{c_1, c_2, \ldots, c_L\} \quad (49)$$

This case describes Tomlinson-Harashima precoding [18, 5] with optimization over $L$ different representations for each information bit. An example of such a respresentation for integer lattice points is shown in Fig. 1. The boundary points

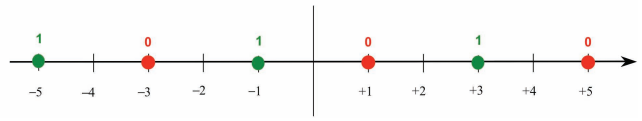


**Figure 1: 2 one-dimensional equally spaced integer lattices representing the two binary states 0 and 1, respectively.**

of the Voronoi regions are

$$v_i = \frac{c_i + c_{i-1}}{2} \quad (50)$$

and the fixed-point equations for $q$ and $b$ become

$$q = \frac{1}{\sqrt{2\pi}} \sum_{i=1}^{L} \int_{\frac{\sqrt{2}R(-b)v_i}{\sqrt{qR'(-b)}}}^{\frac{\sqrt{2}R(-b)v_{i+1}}{\sqrt{qR'(-b)}}} c_i^2\,\mathrm{e}^{-\frac{z^2}{2}}\,\mathrm{d}z \quad (51)$$

$$= c_1^2 + \sum_{i=2}^{L} (c_i^2 - c_{i-1}^2)\,\mathrm{Q}\left(\frac{R(-b)(c_i + c_{i-1})}{\sqrt{2qR'(-b)}}\right) \quad (52)$$

$$b = \frac{\sum_{i=2}^{L} (c_i - c_{i-1}) \exp\left(-\frac{R^2(-b)(c_i+c_{i-1})^2}{4qR'(-b)}\right)}{\sqrt{4\pi qR'(-b)}}. \quad (53)$$

For the case of no precoding at all, i.e. $L = 1$, we get

$$b = 0 \quad (54)$$

$$q = c_1^2 \quad (55)$$

$$E_\mathrm{s} = c_1^2 R(0). \quad (56)$$

### 5.1 Marchenko-Pastur Law

Let $\boldsymbol{H}$ be an $N \times K$ random matrix composed of independent identically distributed entries with variance $1/N$. Then the eigenvalue distribution of

$$\boldsymbol{R} = \boldsymbol{H}^\dagger \boldsymbol{H} \quad (57)$$

converges almost surely, as $K = \alpha N \to \infty$ to the Marchenko-Pastur law [19]. This implies

$$R(w) = \frac{1}{1-\alpha w} \quad (58)$$

$$R'(w) = \frac{\alpha}{(1-\alpha w)^2}. \quad (59)$$

Thus, we find

$$E_\mathrm{s} = 0 \qquad \text{if } \lim_{\beta\to\infty} b = \infty. \quad (60)$$

For finite values of $b$, we get

$$q = c_1^2 + \sum_{i=2}^{L} (c_i^2 - c_{i-1}^2)\,\mathrm{Q}\left(\frac{c_i + c_{i-1}}{\sqrt{2q\alpha}}\right) \quad (61)$$

$$b = \frac{1+\alpha b}{\sqrt{4\pi q\alpha}} \sum_{i=2}^{L} (c_i - c_{i-1}) \exp\left(-\frac{(c_i + c_{i-1})^2}{4q\alpha}\right) \quad (62)$$

and

$$E_\mathrm{s} = \frac{q}{(1+\alpha b)^2}. \quad (63)$$

This relationship is plotted in Fig. 2 for the equally spaced

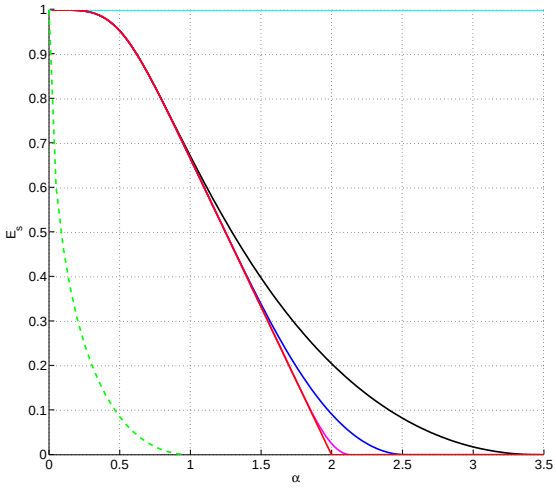


**Figure 2: Load vs. energy per symbol for $L = 1, 2, 3, 6, 100$ shown by the cyan, black, blue, magenta, and red lines, respectively.**

integer lattice

$$\mathcal{B}_{+1} = \{+1, -3, +5, -7, +9, \ldots\} \quad (64)$$

and various numbers of lattice points. The dashed green line shows the lower bound given by $\lambda_\mathrm{min} = (1 - \sqrt{\alpha})^2$, the smallest eigenvalue of $\boldsymbol{R}$. With pre-coding the energy per symbol becomes exactly zero, if the load exceeds a certain threshold. The threshold load is the smaller, the larger the number of lattice points, and reaches $\alpha_\mathrm{t} = 2$ for $L \to \infty$. Beyond the threshold load, the parameter $b$ diverges to infinity. This behavior can be intuitively understood from an

engineering perspective: Since the random matrix $\boldsymbol{R}$ contains zero eigenvalues for $\alpha \geq 1$, pre-coding tries to shape the signal vector $\boldsymbol{x}$ such that is lies within the null-space of $\boldsymbol{R}$. The dimension of the null-space grows with the load. If the load exceed the threshold load, the signal vector can be squeezed into the null-space.

Let us consider the fixed-point equation for $b$ in the limit $b \to \infty$. We find

$$b = \frac{\alpha b}{\sqrt{4\pi q \alpha}} \sum_{i=2}^{L} (c_i - c_{i-1}) \exp\left(-\frac{(c_i + c_{i-1})^2}{4q\alpha}\right). \quad (65)$$

Thus, the solution $b \to \infty$ is stable as long as

$$\sqrt{\frac{\alpha}{4\pi q}} \sum_{i=2}^{L} (c_i - c_{i-1}) \exp\left(-\frac{(c_i + c_{i-1})^2}{4q\alpha}\right) \geq 1. \quad (66)$$

Thus, we find the final result

$$E_{\mathrm{s}} = \begin{cases} 0 & \text{for} \quad \frac{\sqrt{\alpha} \sum_{i=2}^{L} (c_i - c_{i-1})}{\exp\left(\frac{(c_i + c_{i-1})^2}{4q\alpha}\right)} \geq 2\sqrt{\pi q} \\ \frac{q}{(1+\alpha b)^2} & \text{for} \quad \frac{\sqrt{\alpha} \sum_{i=2}^{L} (c_i - c_{i-1})}{\exp\left(\frac{(c_i + c_{i-1})^2}{4q\alpha}\right)} < 2\sqrt{\pi q} \end{cases} \quad (67)$$

The critical value of the load is given for $L = 2$ by

$$\alpha_{\mathrm{t}} \approx 3.4621. \quad (68)$$

## 5.2 Channel Inversion

First we, restrict to the special case of a square channel matrix. The general case is addressed subsequently.

### 5.2.1 Square Channel Matrix

For $\boldsymbol{R} = (\boldsymbol{H}^\dagger \boldsymbol{H})^{-1}$, we find

$$R(w) = \frac{1}{\sqrt{-w}} \quad (69)$$

$$R'(w) = \frac{1}{2(-w)^{\frac{3}{2}}}. \quad (70)$$

Thus, we find

$$E_{\mathrm{s}} \to \infty \qquad \text{if } \lim_{\beta \to \infty} b = 0. \quad (71)$$

For positive values of $b$, we get

$$q = c_1^2 + \sum_{i=2}^{L} \left(c_i^2 - c_{i-1}^2\right) \mathrm{Q}\left(b^{\frac{1}{4}} q^{-\frac{1}{2}} (c_i + c_{i-1})\right) \quad (72)$$

$$b = \frac{b^{\frac{3}{4}}}{\sqrt{2\pi q}} \sum_{i=2}^{L} (c_i - c_{i-1}) \exp\left(-\frac{\sqrt{b}(c_i + c_{i-1})^2}{2q}\right) \quad (73)$$

and

$$E_{\mathrm{s}} = \frac{q}{2\sqrt{b}} \quad (74)$$

which makes the case distinction with respect to the asymptotic behavior of $b$ obsolete. Moreover, we can combine the above 3 equations to find

$$E_{\mathrm{s}} = \pi \left[\frac{c_1^2 + \sum_{i=2}^{L} \left(c_i^2 - c_{i-1}^2\right) \mathrm{Q}\left(\frac{c_i + c_{i-1}}{\sqrt{2E_{\mathrm{s}}}}\right)}{\sum_{i=2}^{L} (c_i - c_{i-1}) \exp\left(-\frac{(c_i + c_{i-1})^2}{4E_{\mathrm{s}}}\right)}\right]^2. \quad (75)$$

Numerical solutions to (75) are shown in Table 1 for the equally spaced integer lattice defined in (64). Obviously, there is little improvement when going from two to three lattice points and negligible improvement for more than 3 lattice points.

**Table 1: Energy per symbol for inverted square channel.**

| $L$ | 1 | 2 | 3 | 4 | $\infty$ |
|---|---|---|---|---|---|
| $E_{\mathrm{s}}$ | $\infty$ | 2.6942 | 2.6656 | 2.6655 | 2.6655 |
| $E_{\mathrm{s}}$ [dB] | $\infty$ | 4.3043 | 4.2579 | 4.2578 | 4.2578 |

### 5.2.2 Rectangular Channel Matrix

For a rectangular channel matrix, the Gramian is only invertible for $\alpha \leq 1$. However, the R-transform is well-defined for any positive aspect ratio. For singular random matrices, the R-transform reflects the fact that the asymptotic eigenvalue distribution has some point mass at infinity. In that case, we find in Appendix B that

$$R(w) = \frac{1 - \alpha - \sqrt{(1-\alpha)^2 - 4\alpha w}}{2\alpha w} \quad (76)$$

$$R'(w) = \frac{\left(1 - \alpha - \sqrt{(1-\alpha)^2 - 4\alpha w}\right)^2}{4\alpha w^2 \sqrt{(1-\alpha)^2 - 4\alpha w}} \quad (77)$$

which for $\alpha = 1$ simplifies to (69) and (70), respectively. It also turns out helpful to recognize that

$$\frac{R^2(w)}{R'(w)} = \frac{\sqrt{(1-\alpha)^2 - 4\alpha w}}{\alpha}. \quad (78)$$

Thus, we find

$$q = c_1^2 + \sum_{i=2}^{L} \left(c_i^2 - c_{i-1}^2\right) \mathrm{Q}\left(\frac{\left((1-\alpha)^2 + 4\alpha b\right)^{\frac{1}{4}} (c_i + c_{i-1})}{\sqrt{2q\alpha}}\right)$$

$$b = \frac{b\sqrt{\frac{\alpha}{\pi q}}\sqrt{(1-\alpha)^2 + 4\alpha b}}{\alpha - 1 + \sqrt{(1-\alpha)^2 + 4\alpha b}} \times \\ \times \sum_{i=2}^{L} (c_i - c_{i-1})\, \mathrm{e}^{-\frac{\sqrt{(1-\alpha)^2 + 4\alpha b}(c_i + c_{i-1})^2}{4q\alpha}}.$$

It is convenient to replace the parameter $b$ by the substitution

$$p = \sqrt{(1-\alpha)^2 + 4\alpha b} \quad (79)$$

which gives

$$q = c_1^2 + \sum_{i=2}^{L} \left(c_i^2 - c_{i-1}^2\right) \mathrm{Q}\left(\sqrt{\frac{p}{2q\alpha}}(c_i + c_{i-1})\right)$$

$$p = 1 - \alpha + \sqrt{\frac{\alpha p}{\pi q}} \sum_{i=2}^{L} (c_i - c_{i-1}) \exp\left(-\frac{p(c_i + c_{i-1})^2}{4q\alpha}\right)$$

and

$$E_{\mathrm{s}} = \frac{q}{p}. \quad (80)$$

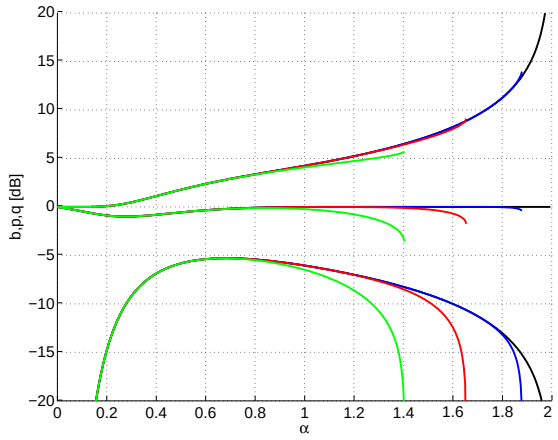


**Figure 3: The macroscopic parameters $q$ (upper lines), $b$ (lower lines), and $p$ (medium lines) versus the load $\alpha$ for $L = 2, 3, 6, 100$. shown by green, red, blue, and black lines, respectively.**

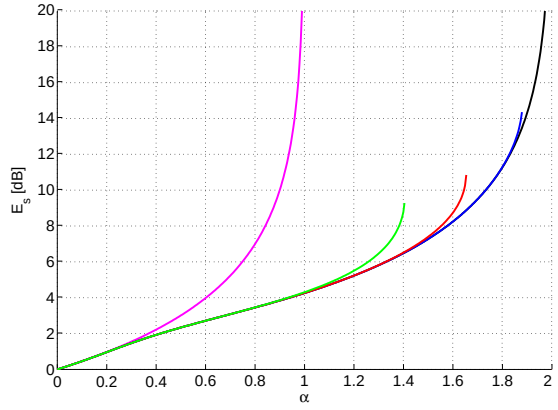


**Figure 4: The transmitted energy per symbol versus the load for $L = 1, 2, 3, 6, 100$ shown by the magenta, green, red, blue, and black lines, respectively.**

Finally, combining the last three equations, we get

$$E_{\mathrm{s}} = \frac{c_1^2 + \sum_{i=2}^{L} \left(c_i^2 - c_{i-1}^2\right) \mathrm{Q}\left(\frac{c_i + c_{i-1}}{\sqrt{2\alpha E_{\mathrm{s}}}}\right)}{1 - \alpha + \sqrt{\frac{\alpha}{\pi E_{\mathrm{s}}}} \sum_{i=2}^{L} \left(c_i - c_{i-1}\right) \exp\left(-\frac{(c_i + c_{i-1})^2}{4\alpha E_{\mathrm{s}}}\right)} \tag{81}$$

The solutions of these fixed-point equations are shown by the solid lines in Fig. 3. Clearly for small load, the parameter $q$ tends to 1, as in that case, no gain due to pre-coding is possible and the symbol with smallest magnitude is preferred. The minimum of the transmit power is shown by the solid line in Fig. 4. Note that precoding enables to achieved finite transmitted energy per symbol even if the channel matrix is singular. This effect has already been explained for Marchenko-Pastur distributed random matrices. Unlike the curve without precoding, the curves for $L > 1$ do not have poles at the threshold load. Instead, a phase transition occurs and the energy per symbol jumps discontinuously from a finite value to infinity.

# 6. 2-D QUADRATURE LATTICE

Consider now the following case:

$$\mathcal{S} = \{00, 01, 10, 11\} \tag{82}$$

$$\mathcal{B}_{1y} = -\mathcal{B}_{0y}^* \qquad \forall y \in \{0, 1\} \tag{83}$$

$$\mathcal{B}_{x1} = +\mathcal{B}_{x0}^* \qquad \forall x \in \{0, 1\} \tag{84}$$

This case extends the one-dimensional pre-coding of binary phase-shift keying (BPSK) on the real line to two-dimensional pre-coding of quaternary phase-shift keying (QPSK) in the complex plane such that Gray mapping is applied and we can consider the pre-coding for QPSK as independent pre-coding of BPSK in both quadrature components.

The symmetry in both quadrature components implies that

$$q = \sqrt{\frac{2}{\pi}} \int_{\mathbb{R}} \left| \operatorname*{argmin}_{x \in \Re\{\mathcal{B}_{1+\mathrm{j}}\}} \left| z\sqrt{\frac{qR'(-b)}{2R^2(-b)}} - x \right| \right|^2 \mathrm{e}^{-\frac{z^2}{2}} \mathrm{d}z \tag{85}$$

$$b = \int_{\mathbb{R}} \operatorname*{argmin}_{x \in \Re\{\mathcal{B}_{1+\mathrm{j}}\}} \left| z\sqrt{\frac{qR'(-b)}{2R^2(-b)}} - x \right| \frac{z\,\mathrm{e}^{-\frac{z^2}{2}} \mathrm{d}z}{\sqrt{\pi q R'(-b)}}. \tag{86}$$

Compared to the one-dimensional case, the only difference is that the right hand sides of the two fixed point equations are multiplied by a factor of 2 which stems from adding the contributions of both quadrature components.

## 6.1 Marchenko-Pastur Law

Using the same convention for the notation of the lattice points as in Subsection 5.1, we find easily that (63) remains valid and $b$ and $q$ are given by

$$q = 2c_1^2 + 2\sum_{i=2}^{L} \left(c_i^2 - c_{i-1}^2\right) \mathrm{Q}\left(\frac{c_i + c_{i-1}}{\sqrt{2q\alpha}}\right) \tag{87}$$

$$b = \frac{1 + \alpha b}{\sqrt{\pi q \alpha}} \sum_{i=2}^{L} \left(c_i - c_{i-1}\right) \exp\left(-\frac{(c_i + c_{i-1})^2}{4q\alpha}\right). \tag{88}$$

In order to make a fair comparison to BPSK, we shall introduce the energy-per bit

$$E_{\mathrm{b}} = \frac{E_{\mathrm{s}}}{\log_2 |\mathcal{S}|}. \tag{89}$$

Note that on the right hand sides of the fixed point equations, $b$ and $q$ only occur as products with the load $\alpha$. Thus, we find the functional relationship

$$E_{\mathrm{b}}^{\mathrm{QPSK,2-dim}}(\alpha) = E_{\mathrm{b}}^{\mathrm{BPSK,1-dim}}(2\alpha). \tag{90}$$

Thus, using complex pre-coding for QPSK instead of real-valued pre-coding for BPSK, we just re-scale the load-axis by a factor of one half.

## 6.2 Channel Inversion

Using the same argumentation about de-coupling between quadrature components, as for the Marchenko-Pastur law,

we find that (80) remains valid and $p$ and $q$ are given by

$$q = 2c_1^2 + 2\sum_{i=2}^{L}(c_i^2 - c_{i-1}^2)\,\mathrm{Q}\left(\sqrt{\frac{p}{2q\alpha}}(c_i + c_{i-1})\right) \quad (91)$$

$$p = 1 - \alpha + \sqrt{\frac{4\alpha p}{\pi q}}\sum_{i=2}^{L}(c_i - c_{i-1})\,\mathrm{e}^{-\frac{p(c_i+c_{i-1})^2}{4q\alpha}}. \quad (92)$$

The solutions to these fixed point equations are shown in Fig. 5. Remarkably, the energy per bit remains as small as

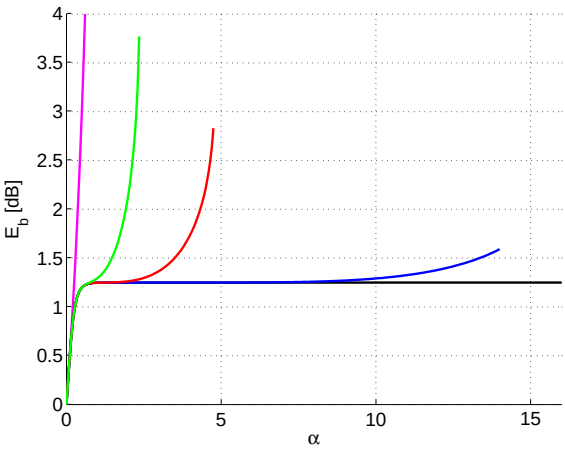


**Figure 5: Transmitted energy per bit versus the load for channel inversion and pre-coding for Gray-mapped QPSK with $L = 1, 2, 3, 6, 100$ shown by the magenta, green, blue, and black lines respectively.**

$E_\mathrm{b} = \frac{4}{3}$ for any load if $L$ grows large.

## 7. 2-D CHECKERBOARD LATTICE

Let

$$\mathcal{S} = \{0, 1\} \quad (93)$$

$$\mathcal{B}_1 = \mathrm{j}\mathcal{B}_0 \subset \mathbb{C}. \quad (94)$$

This case extends the one-dimensional pre-coding of BPSK on the real line to two-dimensional pre-coding of BPSK in the complex plane.

Consider a mapping that looks like a checkerboard where the sets $\mathcal{B}_1$ and $\mathcal{B}_0$ correspond to the black and white fields, respectively. For such a mapping, the boarderlines of the Voronoi regions are not parallel to the real and imaginary axes but intersect these by an angle of 45°.

Considering an unconstrained lattice, i.e. infinitly many lattice points, we can rotate the lattice by 45° degrees without loss of generality due to the rotational invariance of the complex Gaussian integral kernel in the fixed-point equations for $b$ and $q$. After rotation we find the same lattice as in the two-dimensional quadrature precoding except for a lattice scaling by a factor of $1/\sqrt{2}$. Thus, the energy per symbol will be half the energy per symbol of quadrature precoding and the energy per bit will be identical.

## 8. 2-D SEMI-DISCRETE LATTICE

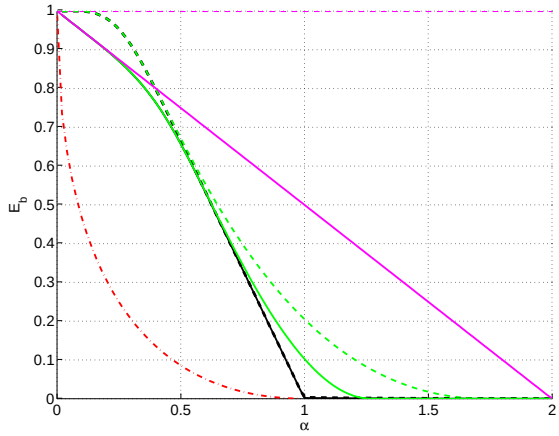


**Figure 6: Energy per bit versus load for precoding with complex quadrature lattice (dashed lines) and semi-discrete lattice (solid lines) for $L = 1, 2, 100$ shown by the magenta, green and black lines, respectively.**

Let

$$\mathcal{S} = \{0, 1, \} \quad (95)$$

$$\mathcal{B}_1 = -\mathcal{B}_0 \subset \mathbb{C}. \quad (96)$$

Moreover, let the imaginary parts of the symbols in $\mathcal{B}_x$ be arbitrary. Thus, we find

$$q = \frac{qR'(-b)}{2R^2(-b)} + \int_{\mathbb{R}} \left| \underset{x\in\Re\{\mathcal{B}_1\}}{\operatorname{argmin}} \left| z\sqrt{\frac{qR'(-b)}{2R^2(-b)}} - x \right| \right|^2 \frac{\mathrm{e}^{-\frac{z^2}{2}}\mathrm{d}z}{\sqrt{2\pi}} \quad (97)$$

$$b = \frac{1}{2R(-b)} + \int_{\mathbb{R}} \underset{x\in\Re\{\mathcal{B}_1\}}{\operatorname{argmin}} \left| z\sqrt{\frac{qR'(-b)}{2R(-b)^2}} - x \right| \frac{z\,\mathrm{e}^{-\frac{z^2}{2}}\mathrm{d}z}{\sqrt{4\pi qR'(-b)}}. \quad (98)$$

### 8.1 Marchenko-Pastur Law

For the Marchenko-Pastur law, we have

$$\frac{R'(-b)}{R^2(-b)} = \alpha. \quad (99)$$

This enables us to easily solve the fixed point equations. For the case $L = 1$, we find

$$E_\mathrm{s} = 1 - \frac{\alpha}{2} \qquad \forall \alpha \leq 2. \quad (100)$$

Fig. 6 compares the complex semi-discrete lattice with complex quadrature lattice in terms of energy per bit. While there is little gain by the semi-discrete lattice in the vicinity of $\alpha = \frac{1}{2}$, there is a noticeable reduction of energy for smaller and larger loads.

### 8.2 Channel Inversion

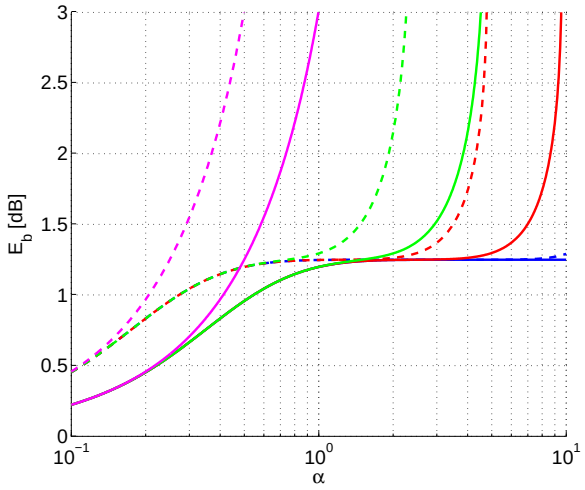


**Figure 7: Energy per bit versus load for precoding with complex quadrature lattice (dashed lines) and semi-discrete lattice (solid lines) for $L = 1, 2, 3, 6$ shown by the magenta, green, red, and blue lines, respectively.**

For channel inversion, we have

$$\frac{R'(-b)}{R^2(-b)} = \frac{\alpha}{p}. \tag{101}$$

This enables us to easily solve the fixed point equations.

Fig. 7 compares the complex semi-discrete lattice with complex quadrature lattice in terms of energy per bit. Precoding with semi-discrete lattices achieves a remarkable gain which comes at the expense of reduced data rate. It is particularly worth to remark that the semi-discrete lattice with $L = 1$ outperforms all quadrature lattices for small loads although its pre-coding procedure has only polynomial complexity. For large loads and large lattice size, the energy per bit approaches $E_\mathrm{b} = \frac{4}{3}$.

## 9. CONCLUSIONS

We found that vector pre-coding can significantly reduce the required transmitted power. In fact, with appropriate precoding, the transmitted power stays always finite. Moreover, we found strong advantages of complex-valued pre-coding over real-valued pre-coding and a trade-off between data rate and required transmit power.

We are aware of the fact that replica symmetry might not hold. Therefore, we have started investigating first order replica symmetry breaking (1RSB). The quantitative analysis is not finished yet, but qualitatively, the results remain unchanged for 1RSB.

## 10. ACKNOWLEDGMENTS

This research was supported by the Research Council of Norway, the National Science Foundation, DARPA, and the European Commission under grants 171133/V30, CCF-0644344, W911NF-07-1-0028, and MIRG-CT-2005-030833, resp.

## 11. REFERENCES

[1] G. Caire, R. R. Müller, and T. Tanaka. Iterative multiuser joint decoding: Optimal power allocation and low-complexity implementation. *IEEE Transactions on Information Theory*, 50(9):1950–1973, Sept. 2004.

[2] M. Debbah and R. Müller. MIMO channel modelling and the principle of maximum entropy. *IEEE Transactions on Information Theory*, 51(5):1667–1690, May 2005.

[3] D. Guo. Performance of multicarrier CDMA in frequency-selective fading via statistical physics. *IEEE Transactions on Information Theory*, 52(4):1765–1774, Apr. 2006.

[4] D. Guo and S. Verdú. Randomly spread CDMA: Asymptotics via statistical physics. *IEEE Transactions on Information Theory*, 51(6):1983–2010, June 2005.

[5] H. Harashima and H. Miyakawa. Matched-transmission technique for channels with intersymbol interference. *IEEE Transactions on Communications*, COM-20:774–780, Aug. 1972.

[6] B. M. Hochwald, C. Peel, and A. Swindlehurst. A vector-perturbation technique for near-capacity multiantenna multiuser communication-Part II: Perturbation. *IEEE Transactions on Communications*, 53(3):537–544, Mar. 2005.

[7] C. Itzykson and J. Zuber. The planar approximation(II). *Journal of Mathematical Physics*, 21(3):411–421, Mar. 1980.

[8] Y. Kabashima. A CDMA multiuser detection algorithm on the basis of belief propagation. *Journal of Physics A: Mathematical and General*, 36:11111–11121, 2003.

[9] H. Li and H. V. Poor. Impact of channel estimation errors on multiuser detection via the replica method. *EURASIP Journal on Wireless Communications and Networking*, 2005(2):175–186, 2005.

[10] E. Marinari, G. Parisi, and F. Ritort. Replica field theory for deterministic models (II): A non-random spin glass with glassy behavior. *Journal of Physics A: Mathematical and General*, 27:7647–7668, 1994.

[11] M. Mezard, G. Parisi, and M. A. Virasoro. *Spin Glass Theory and Beyond*. World Scientific, Singapore, 1987.

[12] R. R. Müller. Applications of large random matrices in communications engineering. In *Proc. of International Conference on Advances in the Internet, Processing, Systems, and Interdisciplinary Research (IPSI)*, Sveti Stefan, Montenegro, Oct. 2003.

[13] R. R. Müller. Channel capacity and minimum probability of error in large dual antenna array systems with binary modulation. *IEEE Transactions on Signal Processing*, 51(11):2821–2828, Nov. 2003.

[14] R. R. Müller and W. H. Gerstacker. On the capacity loss due to separation of detection and decoding. *IEEE Transactions on Information Theory*, 50(8):1769–1778, Aug. 2004.

[15] T. Tanaka. A statistical mechanics approach to large-system analysis of CDMA multiuser detectors. *IEEE Transactions on Information Theory*, 48(11):2888–2910, Nov. 2002.

[16] T. Tanaka and M. Okada. Approximate belief propagation, density evolution, and statistical

neurodynamics for CDMA multiuser detection. *IEEE Transactions on Information Theory*, 51(2):700–706, Feb. 2005.

[17] T. Tanaka and D. Saad. A statistical-mechanics analysis of coded CDMA with regular LDPC codes. In *Proc. of IEEE International Symposium on Information Theory (ISIT)*, page 444, Yokohama, Japan, June/July 2003.

[18] M. Tomlinson. New automatic equaliser employing modulo arithmetic. *IEE Electronics Letters*, 7:138–139, Mar. 1971.

[19] A. M. Tulino and S. Verdú. Random matrix theory and wireless communications. *Foundations and Trends in Communications and Information Theory*, 1(1), June 2004.

[20] D. V. Voiculescu, K. J. Dykema, and A. Nica. *Free Random Variables*. American Mathematical Society, Providence, RI, 1992.

[21] C.-K. Wen and K.-K. Wong. Asymptotic analysis of spatially correlated MIMO multiple-access channels with arbitrary signaling inputs for joint and separate decoding. *Submitted to IEEE Transactions on Information Theory*, 2004.

# APPENDIX

## A. ITZYKSON-ZUBER INTEGRAL

Define

$$Z_{\boldsymbol{D}}(s) = \frac{1}{N}\sum_{k=0}^{\infty} s^{k+1}\mathrm{tr}\,\boldsymbol{D}^k = -\int \frac{\mathrm{dP}_{\boldsymbol{D}}(x)}{x-\frac{1}{s}} = -m_{\boldsymbol{D}}\left(s^{-1}\right) \quad (102)$$

with $m_{\boldsymbol{D}}(\cdot)$ denoting the Stieltjes transform of the distribution of $\boldsymbol{D}$. Following the approach by Itzykson and Zuber [7], Marinari et al. [10] show that with $\boldsymbol{O}$ being $K \times K$ and Haar distributed, $\boldsymbol{D}$ diagonal, and $\boldsymbol{F}$ having finite rank and non-zero eigenvalues $\lambda_1, \ldots, \lambda_n$, we have

$$\int \exp\left(\mathrm{tr}\,\boldsymbol{O}\boldsymbol{F}\boldsymbol{O}^\dagger\boldsymbol{D}\right)\mathrm{d}\boldsymbol{O} = \exp\left(K\sum_{a=1}^{n} G_{\boldsymbol{D}}\left(\lambda_a\right)\right) \quad (103)$$

with

$$G_{\boldsymbol{D}}(\lambda) = \int_0^1 \frac{\psi_{\boldsymbol{D}}(\lambda w)-1}{w}\,\mathrm{d}w \quad (104)$$

and the function $\psi_{\boldsymbol{D}}(\cdot)$ being defined as

$$\psi_{\boldsymbol{D}}(w) = \frac{w}{Z_{\boldsymbol{D}}^{-1}(w)} \quad (105)$$

where $Z_{\boldsymbol{D}}^{-1}(w)$ is the inverse of $Z_{\boldsymbol{D}}(w)$ with respect to composition, i.e. $Z_{\boldsymbol{D}}^{-1}(Z_{\boldsymbol{D}}(w)) = w$. Thus, we find

$$\begin{aligned}
\psi_{\boldsymbol{D}}\left(Z_{\boldsymbol{D}}(w)\right) &= \frac{Z_{\boldsymbol{D}}(w)}{w} && (106)\\
\psi_{\boldsymbol{D}}\left(-m_{\boldsymbol{D}}\left(w^{-1}\right)\right) &= \frac{-m_{\boldsymbol{D}}\left(w^{-1}\right)}{w} && (107)\\
\psi_{\boldsymbol{D}}\left(-m_{\boldsymbol{D}}\left(w\right)\right) &= -wm_{\boldsymbol{D}}\left(w\right) && (108)\\
\psi_{\boldsymbol{D}}\left(-w\right) &= -wm_{\boldsymbol{D}}^{-1}\left(w\right) && (109)\\
\psi_{\boldsymbol{D}}\left(w\right) &= wm_{\boldsymbol{D}}^{-1}\left(-w\right) && (110)\\
&= w\left(R_{\boldsymbol{D}}(w)+w^{-1}\right) && (111)\\
&= 1+wR_{\boldsymbol{D}}(w) && (112)\\
\frac{\psi_{\boldsymbol{D}}(\lambda w)-1}{w} &= \lambda R_{\boldsymbol{D}}(\lambda w) && (113)
\end{aligned}$$

with the R-transform defined as [20]

$$R_{\boldsymbol{D}}(w) = m_{\boldsymbol{D}}^{-1}(-w) - \frac{1}{w}. \quad (114)$$

Thus, we find for the Itzykson-Zuber integral

$$\begin{aligned}
&\int \exp\left(\mathrm{tr}\,\boldsymbol{O}\boldsymbol{F}\boldsymbol{O}^\dagger\boldsymbol{D}\right)\mathrm{d}\boldsymbol{O} && (115)\\
&\quad= \exp\left(K\sum_{a=1}^{n}\lambda_a\int_0^1 R_{\boldsymbol{D}}\left(\lambda_a w\right)\mathrm{d}w\right) && (116)\\
&\quad= \exp\left(K\sum_{a=1}^{n}\int_0^{\lambda_a} R_{\boldsymbol{D}}\left(w\right)\mathrm{d}w\right) && (117)
\end{aligned}$$

## B. INVERSE MARCHENO-PASTUR LAW

Let $\mathrm{p}_X(x)$ be an arbitrary pdf such that the Stieltjes transforms

$$m_X(s) = \int \frac{\mathrm{dP}_X(x)}{x-s} \quad (118)$$

and

$$m_{X^{-1}}(s) = \int \frac{\mathrm{dP}_X(x)}{\frac{1}{x}-s} \quad (119)$$

exist for some complex $s$ with $\Im(s) > 0$. It can easily be checked that

$$m_{X^{-1}}\left(\frac{1}{s}\right) = -s\left(1+sm_X(s)\right). \quad (120)$$

Let $s = m_X^{-1}(-w)$. Then, we find

$$m_{X^{-1}}\left(\frac{1}{m_X^{-1}(-w)}\right) = -m_X^{-1}(-w)\left(1-wm_X^{-1}(-w)\right). \quad (121)$$

and

$$\frac{1}{m_X^{-1}(-w)} = m_{X^{-1}}^{-1}\left(-m_X^{-1}(-w)\left(1-wm_X^{-1}(-w)\right)\right). \quad (122)$$

With (114), we find

$$\begin{aligned}
\frac{1}{R_X(w)+\frac{1}{w}} &= R_{X^{-1}}\left(-wR_X(w)\left(R_X(w)+\frac{1}{w}\right)\right)\\
&\quad -\frac{1}{wR_X(w)\left(R_X(w)+\frac{1}{w}\right)} && (123)
\end{aligned}$$

and

$$\frac{1}{R_X(w)} = R_{X^{-1}}\left(-R_X(w)\left(1+wR_X(w)\right)\right). \quad (124)$$

It is well known that for an $N \times \alpha N$ random matrix $\boldsymbol{H}$ with i.i.d. entries of variance $(\alpha N)^{-1}$, the R-transform of the limiting spectral measure $\mathrm{P}_{\boldsymbol{H}^\dagger\boldsymbol{H}}(x)$ is given by

$$R_{\boldsymbol{H}^\dagger\boldsymbol{H}}(w) = \frac{1}{1-\alpha w}. \quad (125)$$

Letting $X^{-1} = \boldsymbol{H}^\dagger\boldsymbol{H}$, we find

$$R_{(\boldsymbol{H}^\dagger\boldsymbol{H})^{-1}}(w) = 1+\alpha R_{(\boldsymbol{H}^\dagger\boldsymbol{H})^{-1}}(w)\left(1+wR_{(\boldsymbol{H}^\dagger\boldsymbol{H})^{-1}}(w)\right) \quad (126)$$

with (124). Solving (126) for the R-transform implies (76). Note that for $\alpha \geq 1$, the mean of the spectral measure is diverging. Thus, the R-transform must have a pole at $w = 0$ which excludes the other solution of (126).